

Efficiency Analysis of Solar-Assisted Drying System

Mohit Pauranik¹ and Raj Kumar Yadav²

Department of Mechanical Engineering^{1,2}

Adina Institute of Science and Technology, Sagar, India

yadavr1709@gmail.com

Abstract: *The global surge in food and energy demands necessitates sustainable preservation methods to reduce spoilage, which is often caused by bacterial growth in moisture-laden foods. This study presents a cost-effective solar-assisted greenhouse dryer designed with locally available materials. Tested over three days in forced convection mode, mass flow rates of 0.10, 0.16, and 0.22 kg/s showed average heat gains of 1.69 kW, 2.02 kW, and 2.21 kW, respectively, while average heat losses were 0.62 kW, 0.51 kW, and 0.43 kW. The modifications yielded an R^2 of 0.99, confirming significant efficiency improvements. This dryer offers an eco-friendly, reliable drying alternative.*

Keywords: Solar-assisted greenhouse drying system, no load, heat gain, heat loss, forced circulation, thermal performance.

I. INTRODUCTION

Solar energy has gained prominence in recent decades as a clean, renewable energy source, offering an environmentally friendly alternative to fossil fuels, which are costly, polluting, and finite[1][2]. Developing countries are increasingly adopting solar applications across areas like solar drying, water heating, power generation, and distillation. Drying offers benefits such as extended shelf life, weight reduction, and improved quality, yet faces challenges with energy dependency and potential high initial costs[3][4]. Different drying methods—open sun drying, industrial drying, and solar drying—each have pros and cons. Open sun drying is cost-effective but weather-dependent, industrial drying is fast but costly and energy-intensive, while solar drying offers energy efficiency but depends on sunlight availability[5]. Each method's suitability depends on product type, environmental conditions, and cost. This study focuses on a solar-assisted greenhouse dryer designed to preserve agricultural products by reducing moisture content, preventing spoilage, and conserving energy. Utilizing solar energy for drying extends the safe storage life of commodities, countering high moisture levels that trigger biological spoilage. Heat transfer plays a critical role in optimizing the drying process in these systems.

II. LITERATURE REVIEW

Hossain and Bala[6] designed and constructed the forced-convection greenhouse solar dryer. Their designed dryer efficiently reduced red and green chili moisture levels in 20-22 hours, significantly faster than sun drying, while preserving the chilies' color and pungency, demonstrating its effectiveness and quality retention. Kumar and Kumar[7] noticed that adding an air cavity to a natural convection solar dryer improved its no-load thermal efficiency from 22.68% to 34.08%. Jain et al. [8] found that In the no-load condition, where the dryer operated without any drying material inside, the highest temperature recorded was 77.4 °C with solar reflectors and 59.1 °C without reflectors. This indicates that the solar reflectors significantly increased the internal temperature in no-load conditions, contributing to a higher potential drying efficiency. Morad et al. [9] designed and developed a solar tunnel dryer at Egypt's Mechanization Centre to dry peppermint plants and leaves. Results show drying rates enhanced by 22.78% and 24.8%, respectively, reducing drying times by 9 hours for whole plants and 8 hours for leaves. Nayak and Tiwari[10] were developed a dryer at IIT Delhi and its performance was evaluated using energy and exergy analyses, comparing thermal model predictions with experimental data to enhance drying efficiency. Mahapatra and Tripathy [11] evaluated the no-load thermal efficiency and convective heat transfer coefficient ($h_{c,p-a}$) of direct, indirect, and mixed-mode passive solar

dryers. Tiwari and Kumar [12] studies the GSD and showed that in forced convection, the convective mass coefficient increased by 90% and 135% with higher mass, enhancing drying efficiency. In contrast, natural convection saw a 30% decrease, indicating that mass significantly impacts drying performance differently across methods. Asoegwu and Nwakuba [13] evaluated an Arduino-controlled hybrid solar-electric cabinet dryer under no-load conditions. Kumar [14] installed even span roof type GSD based on active mode at Guru Jambheshwar University of Science and Technology in Hisar, Haryana. It constructed with PVC pipes and had a floor area of 1.2 m × 0.8 m and was covered with a 200-micron UV cover. A fan on the sidewall provided a 5 m/s air velocity. Average convective and evaporative heat transfer coefficients were 0.759 W/m² and 23.48 W/m², respectively.

The introduction emphasizes solar energy's benefits for sustainable agricultural drying, reducing spoilage and energy use, with heat transfer as key. For this purpose, low-cost solar dryers have been designed to provide benefits to the farmer in terms of their hard work, time and money which they invest during the cultivation of crops.

This study evaluates the thermal performance of a low-cost greenhouse solar-assisted dryer over three days in forced convection mode. Testing in no-load conditions assesses its feasibility for farmers, examines performance across varying mass flow rates, identifies suitable crops, evaluates thermal parameters (e.g., heat transfer coefficient), and observes the impact of modifications for future improvements.

III. EXPERIMENTATION

A solar dryer was built at the Adina Institute of Science and Technology. The dryer's side walls are 1.2 m high, with a central height of 2.4 m and a base area of 3.52 m². The roof is inclined at 23.50° and covered with a 3 mm UV-resistant polycarbonate sheet. Two ventilation gaps measuring 0.1 m × 0.1 m are located at the top and rear sections to allow air circulation, supported by a fan (220-230 V, 50 Hz) installed at the upper back wall. Ground temperatures were initially measured on an uncovered floor from October 1–3, 2024, and later on a covered floor from October 6–8, 2024. Air mass flow rates were held at 0.10 kg/s on the first day, 0.16 kg/s on the second, and 0.22 kg/s on the third, consistent across both test conditions.

IV. RESEARCH METHODOLOGY

4.1 Determination of overall heat transfer coefficient

The overall heat transfer value can be determined using several heat transfer parameters, which are discussed below.

4.2.1 Convective heat transfer coefficient from ground to room (h_{gdr}) [15][16][17]

$$h_{gdr} = 0.884 \left(T_{gd} - T_{rm} + \frac{[P(T_{gd}) - \phi P(T_{rm})](T_{gd} - 273)}{268.9 \times 10^3 - P(T_{gd})} \right)^{1/3} \quad (1)$$

4.2.2 Radiative heat transfer coefficient (h_{ra}) [15][16]

$$h_{ra} = \frac{\sigma \varepsilon [(T_{gd} + 273.15)^4 - (T_{rm} + 273.15)^4]}{(T_{gd} - T_{rm})} \quad (2)$$

4.2.3 Overall heat transfer coefficient (U)

The summation of all types of heat transfer coefficients involved throughout the drying process is termed the overall heat transfer coefficient. Mathematically the value of the overall heat transfer coefficient (U) can be expressed as:-

$$\frac{1}{U} = \frac{1}{h'} + \frac{X}{K_c} + \frac{1}{h_{ca}} \quad (3) \quad \text{Where}$$

the value of h' and h_{ca} is calculated with the help of eqn. (4) and (5) as:-

$$h' = h_{gdr} + h_{ra} + h_{ev} \quad (4)$$

$$h_{ca} = 7.2 + 3.8 V_w \quad (5)$$

The value of h_{ev} has been neglected because, for the forced convection in an unload conduction, the evaporative losses are very less.

4.3 Instantaneous thermal loss efficiency factor[16][15]

This value can be determined as follows:-

$$\eta_i = \frac{U \sum A_i (T_{rm} - T_o)}{I A_{gd}} \tag{6}$$

4.4 Heat Gain

Heat gain is defined as the product of the heat capacity and the temperature difference between the room temperature and the ambient temperature. The following relation can determine the heat gain in the greenhouse during the experiment:

$$H_g = m C_p \Delta T \tag{7}$$

V. RESULT AND DISCUSSION

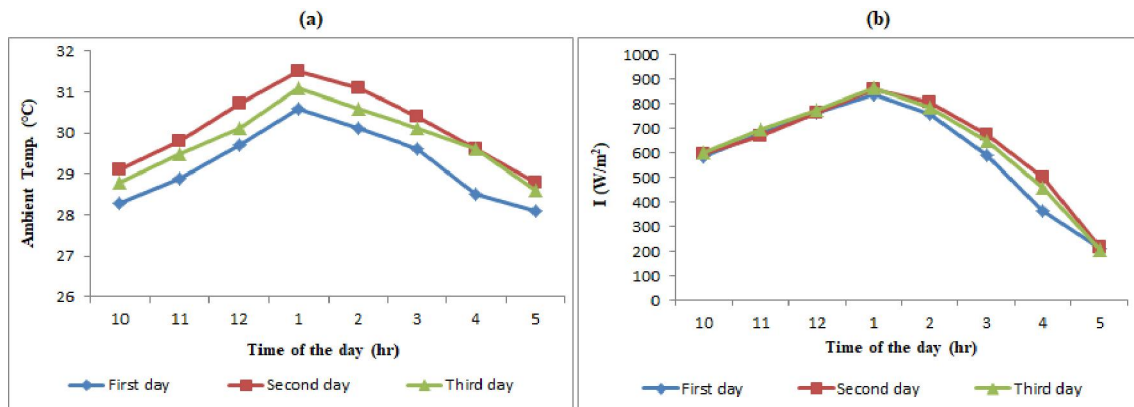


Figure 1 (a) Changes in ambient temperature (b) Variation of solar radiation with time

Figures 1 (a) and (b) illustrate the variation in ambient temperature and solar radiation throughout the day. Weather conditions remained relatively consistent across all experimental days. The maximum temperatures recorded were 30.6°C, 31.5°C, and 31.1°C on initial, subsequent and last days respectively. Ambient conditions play a crucial role in the drying process, as higher ambient temperature and solar radiation result in faster drying. However, since the experiments were conducted in October, both ambient temperature and solar radiation levels were lower compared to the summer season. The recorded solar radiation values ranged from a minimum of 206 W/m² to 215 W/m² and a maximum of 835 W/m² to 856 W/m².

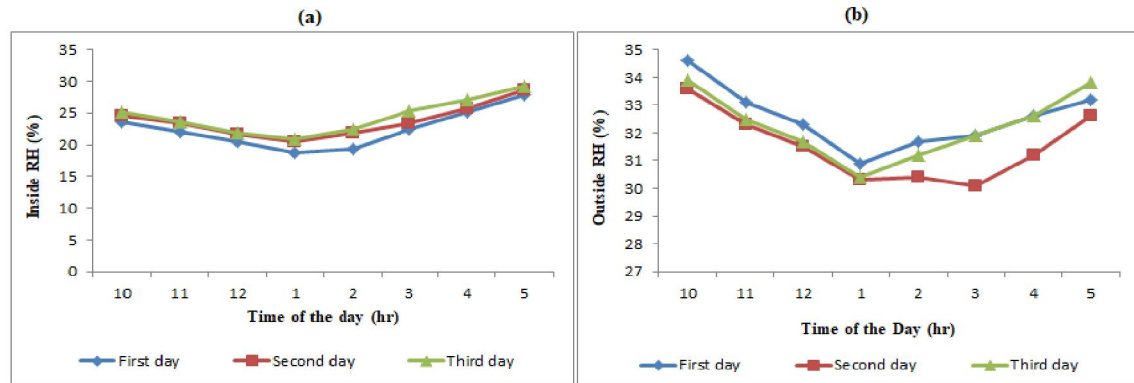


Figure 2 (a) Changes in relative humidity inside the solar assisted GSD (b) Changes in relative humidity outside the solar assisted GSD

Figures 2 (a) and (b) show the variation in relative humidity inside and outside the GSD throughout the day. The minimum relative humidity inside the GSD was recorded as 18.8%, 20.5%, and 20.9%, while outside, it was 30.9%,

30.3%, and 30.4% on days 1, 2, and 3, respectively. Notably, the minimum inside relative humidity was lower than the outside relative humidity by 39.15%, 32.34%, and 31.25% for days 1, 2, and 3, respectively. The increase in minimum relative humidity is attributed to a decrease in room temperature on the respective days, which resulted from an increase in fan velocity, as these two factors are inversely related.

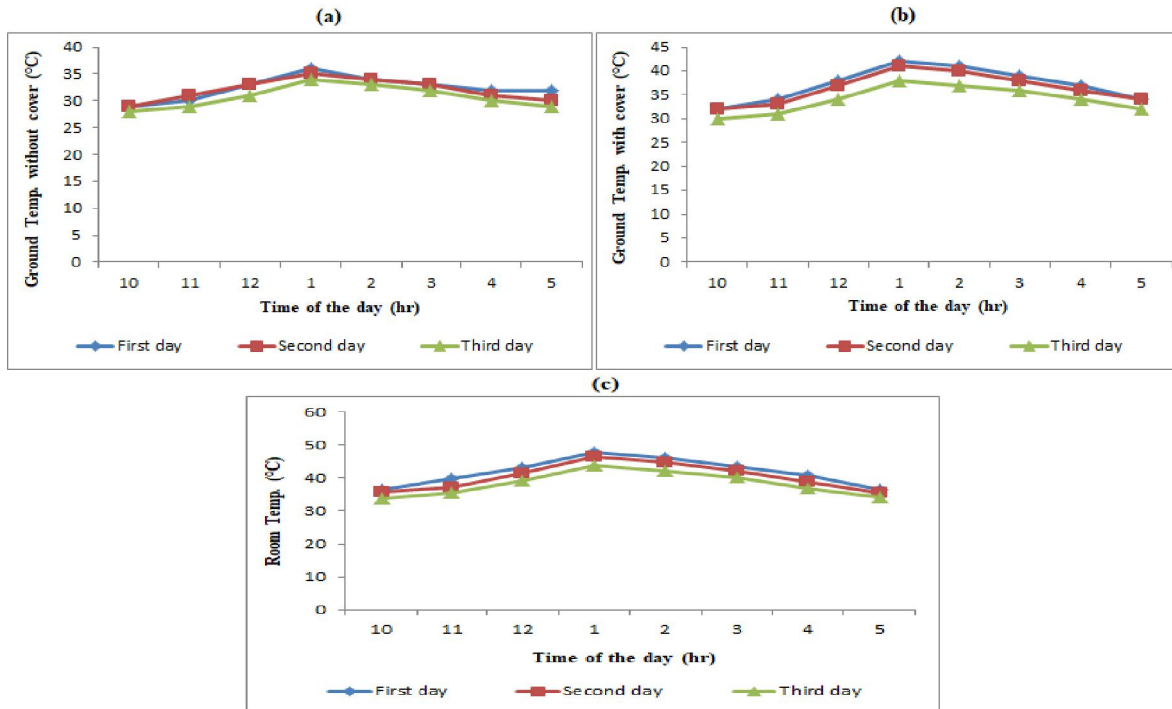
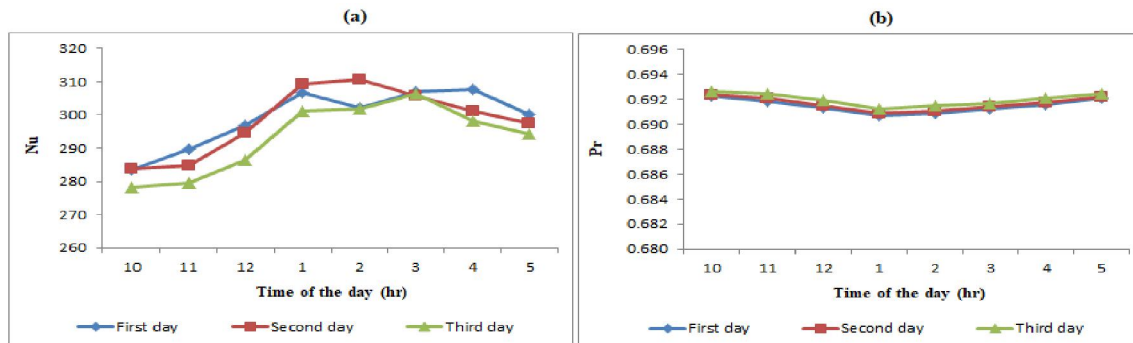


Figure 3(a) Changes in ground temperature with cover (b)Changes in ground temperature without cover (c) Variation of room temperature inside the greenhouse solar dryer

Figures 3 (a) and 3 (b) depict the variation in ground temperature without and with a cover throughout the day under no-load conditions in the GSD. Ground temperature is a key factor that significantly influences the drying process. The results indicate that the maximum ground temperatures without cover were 36°C, 35°C, and 34°C on consecutive days, while with the cover, they increased to 42°C, 41°C, and 38°C on days 1, 2, and 3, respectively.

Figure 3 (c) illustrates the variation in room temperature inside the GSD with a covered floor throughout the day. Under no-load conditions, the room air temperature provides valuable data to determine the appropriate crops for drying inside the greenhouse dryer. The maximum room temperatures recorded under covered conditions were 47.9°C, 46.3°C, and 43.8°C on the consecutive experimental days. These temperatures decreased progressively due to an increase in air velocity over the days. This is because higher air velocity accelerates heat dissipation from inside to outside the GSD, reducing the time available for the dryer to reach the higher temperatures observed under lower velocity conditions.



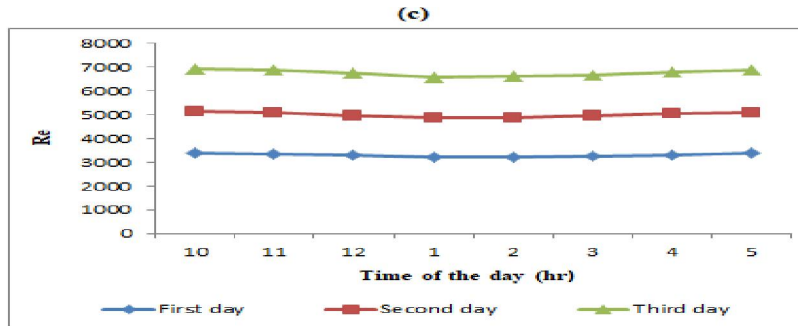


Figure 4 Variation of (a) Nusselt number, (b) Prandtl number and (c) Reynolds number with time of the day

Figure 4 (a) shows the variation of the Nusselt number throughout the day and the ground is covered with a tarpaulin. The Nusselt number ranged from 283.56 to 307.56 on day 1, 283.94 to 310.49 on day 2, and 278.07 to 306.38 on day 3. Figure 4 (b) illustrates the variation of the Prandtl number over time, with a consistent value of 0.692 across all three days. This consistency is due to the fact that the Prandtl number depends on both ambient conditions and fluid properties, which remained nearly constant during the experiment. Figure 4 (c) depicts the variation in the Reynolds number over the course of the day. The average Reynolds numbers for days 1, 2, and 3 were 3312.07, 5000.50, and 6751.30, respectively. In all cases, the Reynolds number exceeded 2300, indicating turbulent flow. As velocity increased, inertia forces became more dominant over viscous forces, leading to higher Reynolds numbers. In greenhouse solar drying, the significance of the Reynolds number lies in its correlation with the rate of heat transfer. A higher Reynolds number indicates more rapid heat and mass transfer from the agricultural products, accelerating the drying process.

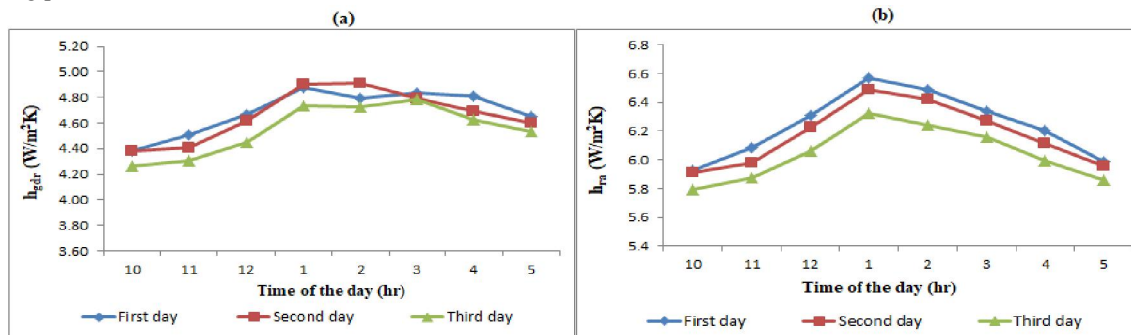


Figure 5(a) Changes in convective heat transfer coefficient from ground to room with time of the day and (b) Variation of radiative heat transfer coefficient from room to air

The convective heat transfer coefficient from ground to room (h_{gdr}), radiative heat transfer coefficient from room to air (h_{ra}), and the overall heat transfer coefficient (U) were calculated using equations 4-8. Figures 5(a) and 5(b) illustrate the variation of these coefficients, showing the convective heat transfer from ground to room and radiative heat transfer from room to air, respectively. The convective heat transfer coefficient is a proportional factor in Newton's law of cooling or heating, representing the rate of convective heat transfer between the fluid medium (hot air inside the greenhouse) and the surface of the crop. The average convective heat transfer coefficient from ground to room was calculated to be 4.69 W/m², 4.66 W/m², and 4.55 W/m² for days 1, 2, and 3, respectively. Meanwhile, the average radiative heat transfer coefficient from room to air was 6.24 W/m², 6.17 W/m², and 6.04 W/m² on the corresponding days.

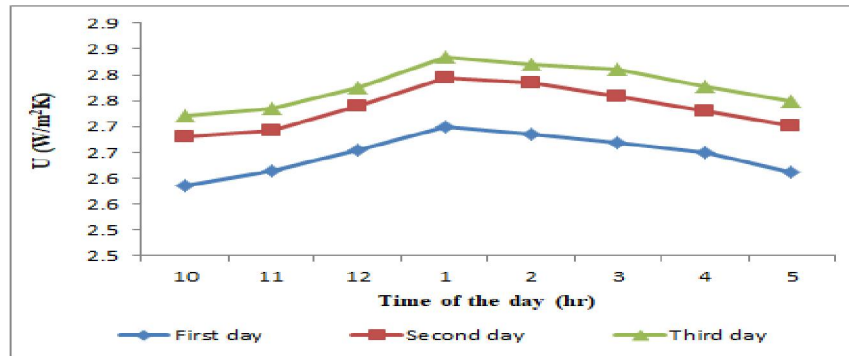


Figure 6 Variation of overall heat loss transfer coefficient with time of the day

Figure 6 illustrates the variation of the overall heat loss transfer coefficient throughout the day. The average values of the overall heat loss transfer coefficient for the three experimental days were 2.65 W/m², 2.73 W/m², and 2.78 W/m², respectively.

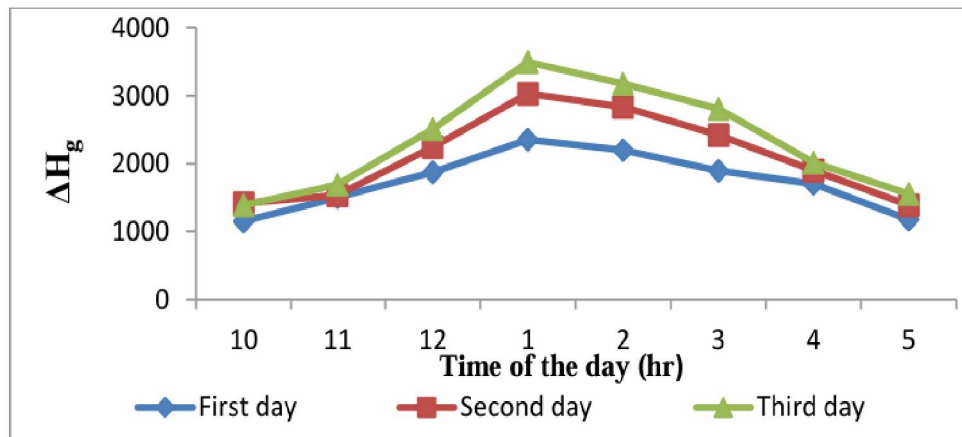


Figure 7 Variation of heat gain concerning time of the day

Figure 7 presents the variation in heat gain inside the greenhouse throughout the experiment. Heat gain is a crucial factor in drying, as it facilitates moisture evaporation from the product's surface. The maximum heat gain recorded was 2353.933 W on the first day 1, 3032.447 W on the second day, and 3498.469 W on the last day. These values highlight the importance of heat gain in enhancing the drying efficiency.

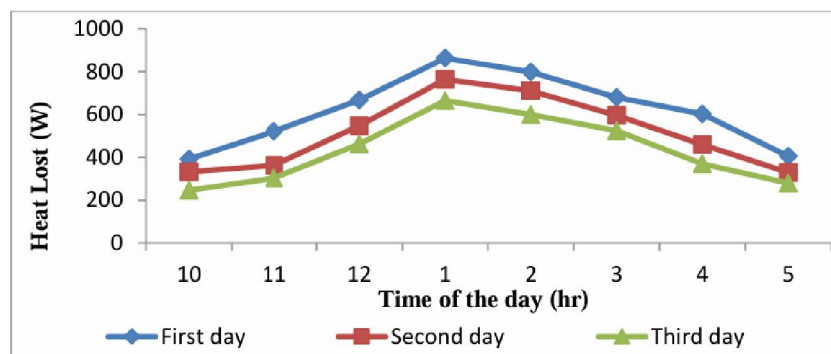


Figure 8 Variation of heat lost to time of the day

Figure 8 illustrates the variation in heat loss throughout the day, which is crucial for evaluating the effectiveness of modifications made to enhance the thermal performance of the GSD. The average heat loss values recorded were 620 W on day 1, 530 W on day 2 and 440 W on day 3. This trend indicates that the decrease in room temperature from day 1 to day 3 directly contributes to the reduction in heat loss, highlighting the relationship between room temperature and heat loss.

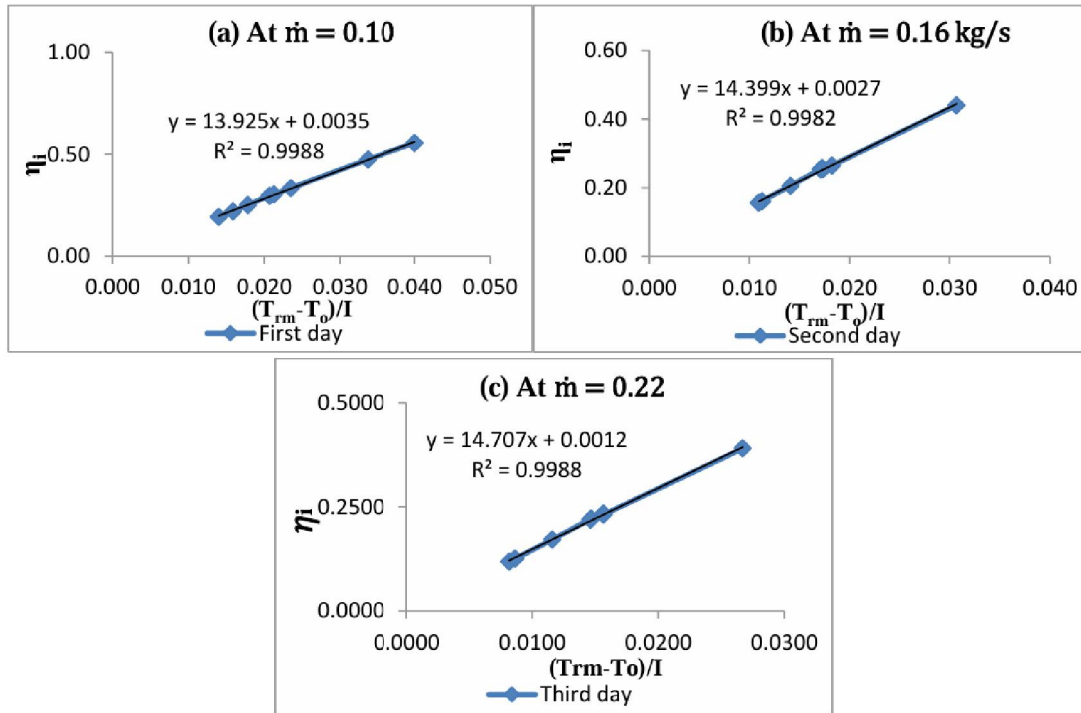


Figure 9 Representation of characteristics curve at (a) $\dot{m} = 0.10$ kg/s, (b) $\dot{m} = 0.16$ kg/s and (c) $\dot{m} = 0.22$ kg/s respectively

Figures 9 (a), (b), and (c) illustrate the variation of the thermal loss efficiency factor (η_i) concerning the ratio of room temperature (T_{rm}) to outside temperature (T_o/I). This characteristic curve is constructed to demonstrate the modifications made to the GSD. The coefficient of determination ($R^2 = 0.99$) confirms the effectiveness of these modifications, as it intercepts the zero point, indicating a strong correlation

VI. CONCLUSION

The experiment conducted over three days in covered floor conditions with varying mass flow rates in forced convection mode yielded the following results:

- The maximum room temperature was consistently higher than the ambient temperature, with differences of 17.3°C, 14.8°C, and 12.7°C on days 1, 2, and 3, respectively, during peak hours.
- The interception of the characteristic curve at zero confirms the modifications made to the GSD.
- The increase in air velocity on consecutive experimental days contributed to a higher average mass flow rate. This increase in mass flow rate enhanced the overall heat transfer coefficient, resulting in a faster drying process.
- The average heat loss values recorded were 0.62 kW, 0.53 kW and 0.44 kW for days 1, 2, and 3, respectively.
- The estimated values of diverse thermal parameters can be used to select appropriate crops for drying applications.

REFERENCES

- [1] T.-Z. Ang, M. Salem, M. Kamarol, H. S. Das, M. A. Nazari, and N. Prabakaran, "A comprehensive study of renewable energy sources: Classifications, challenges and suggestions," *Energy Strateg. Rev.*, vol. 43, p. 100939, Sep. 2022, doi: 10.1016/j.esr.2022.100939.
- [2] J. Wang and W. Azam, "Natural resource scarcity, fossil fuel energy consumption, and total greenhouse gas emissions in top emitting countries," *Geosci. Front.*, vol. 15, no. 2, p. 101757, Mar. 2024, doi: 10.1016/j.gsf.2023.101757.
- [3] A. Lingayat, R. Balijepalli, and V. P. Chandramohan, "Applications of solar energy based drying technologies in various industries – A review," *Sol. Energy*, vol. 229, pp. 52–68, Nov. 2021, doi: 10.1016/j.solener.2021.05.058.
- [4] M. Vera Zambrano, B. Dutta, D. G. Mercer, H. L. MacLean, and M. F. Touchie, "Assessment of moisture content measurement methods of dried food products in small-scale operations in developing countries: A review," *Trends Food Sci. Technol.*, vol. 88, pp. 484–496, Jun. 2019, doi: 10.1016/j.tifs.2019.04.006.
- [5] N. M. Ortiz-Rodríguez, M. Condori, G. Durán, and O. Garcia-Valladares, "Solar drying Technologies: A review and future research directions with a focus on agroindustrial applications in medium and large scale," *Appl. Therm. Eng.*, vol. 215, p. 118993, Oct. 2022, doi: 10.1016/j.applthermaleng.2022.118993.
- [6] M. A. Hossain and B. K. Bala, "Drying of hot chilli using solar tunnel drier," *Sol. Energy*, vol. 81, no. 1, pp. 85–92, Jan. 2007, doi: 10.1016/j.solener.2006.06.008.
- [7] Shimpy, M. Kumar, and A. Kumar, "Experimental and simulation studies on the no-load performance assessment of a domestic solar dryer," *Heat Transf.*, vol. 53, no. 3, pp. 1312–1335, May 2024, doi: 10.1002/htj.22994.
- [8] R. Jain, A. S. Paul, D. Sharma, and N. L. Panwar, "Enhancement in thermal performance of solar dryer through conduction mode for drying of agricultural produces," *Energy Nexus*, vol. 9, p. 100182, Mar. 2023, doi: 10.1016/j.nexus.2023.100182.
- [9] M. M. Morad, M. A. El-Shazly, K. I. Wasfy, and H. A. M. El-Maghawry, "Thermal analysis and performance evaluation of a solar tunnel greenhouse dryer for drying peppermint plants," *Renew. Energy*, vol. 101, pp. 992–1004, Feb. 2017, doi: 10.1016/j.renene.2016.09.042.
- [10] S. Nayak and G. N. Tiwari, "Energy and exergy analysis of photovoltaic/thermal integrated with a solar greenhouse," *Energy Build.*, vol. 40, no. 11, pp. 2015–2021, Jan. 2008, doi: 10.1016/j.enbuild.2008.05.007.
- [11] A. Mahapatra and P. P. Tripathy, "Thermal performance analysis of natural convection solar dryers under no load condition: experimental investigation and numerical simulation," *Int. J. Green Energy*, vol. 16, no. 15, pp. 1448–1464, Dec. 2019, doi: 10.1080/15435075.2019.1671417.
- [12] A. Kumar and G. N. Tiwari, "Effect of mass on convective mass transfer coefficient during open sun and greenhouse drying of onion flakes," *J. Food Eng.*, vol. 79, no. 4, pp. 1337–1350, Apr. 2007, doi: 10.1016/j.jfoodeng.2006.04.026.
- [13] N. R. Nwakuba, C. O. Chukwuezie, S. N. Asoegwu, and K. N. Nwaigwe, "No-Load Performance Testing of an Arduino-Primed Hybrid Solar-Electric Crop Dryer," in *2017 Spokane, Washington July 16 - July 19, 2017*, 2017, doi: 10.13031/aim.201700079.
- [14] M. Kumar, "Forced convection greenhouse papad drying: An experimental study," *J. Eng. Sci. Technol.*, vol. 8, no. 2, pp. 177–189, 2013.
- [15] G. N. T. Barnwal, P., *Fundamentals of solar dryers*. New Delhi: Anamaya Publishers, 2008.
- [16] G. N. Tiwari, S. Kumar, and O. Prakash, "Evaluation of convective mass transfer coefficient during drying of jaggery," *J. Food Eng.*, vol. 63, no. 2, pp. 219–227, Jun. 2004, doi: 10.1016/j.jfoodeng.2003.07.003.
- [17] Shyam, I. M. Al-Helal, A. K. Singh, and G. N. Tiwari, "Performance evaluation of photovoltaic thermal greenhouse dryer and development of characteristic curve," *J. Renew. Sustain. Energy*, vol. 7, no. 3, May 2015, doi: 10.1063/1.4921408.